Characterizing Replication Intermediates in the Amplified CHO Dihydrofolate Reductase Domain by Two Novel Gel Electrophoretic Techniques

ROBERT F. KALEJTA,[1,2] HONG-BO LIN,[1] PIETER A. DIJKWEL,[1] AND JOYCE L. HAMLIN[1,2*]

Department of Biochemistry[1] and Cell and Molecular Biology Program,[2] University of Virginia School of Medicine, Charlottesville, Virginia 22908

Using neutral/neutral and neutral/alkaline two-dimensional (2-D) gel techniques, we previously obtained evidence that initiation can occur at any of a large number of sites distributed throughout a broad initiation zone in the dihydrofolate reductase (DHFR) domain of Chinese hamster ovary (CHO) cells. However, other techniques have suggested a much more circumscribed mode of initiation in this locus. This dichotomy has raised the issue whether the patterns of replicating DNA on 2-D gels have been misinterpreted and, in some cases, may represent such noncanonical replication intermediates as broken bubbles or microbubbles. In an accompanying study (R. F. Kalejta and J. L. Hamlin, Mol. Cell. Biol. 16:4915–4922, 1996), we have shown that broken bubbles migrate to unique positions in three different gel systems and therefore are not likely to be confused with classic replication intermediates. Here, we have applied a broken bubble assay developed from that study to an analysis of the amplified DHFR locus in CHO cells. This assay gives information about the number and positions of initiation sites within a fragment. In addition, we have analyzed the DHFR locus by a novel stop-and-go-alkaline gel technique that measures the size of nascent strands at all positions along each arc in a neutral/neutral 2-D gel. Results of these analyses support the view that the 2-D gel patterns previously assigned to classic, intact replication bubbles and single-forked structures indeed correspond to these entities. Furthermore, potential nascent-strand start sites appear to be distributed at very frequent intervals along the template in the intergenic region in the DHFR domain.

Because of the great complexity of higher eukaryotic genomes, the identification of origins of replication has proven to be extremely challenging. In the absence of a reliable genetic assay for identifying autonomously replicating sequence elements, several origin mapping strategies have been devised to localize start sites in a region of interest, with the assumption that the responsible genetic element (replicator) will lie close by. The Chinese hamster dihydrofolate reductase (DHFR) replicon (Fig. 1A) has been analyzed by almost every available replicon mapping method, and all methods suggest that an origin lies somewhere in the 55-kb spacer region between the DHFR and 2BE2121 genes (reviewed in references 8, 13, and 25). However, different methods of analysis have not provided an entirely coherent picture of initiation in this locus. For example, results from high-resolution intrinsic labelling in the early S period (1, 9, 23, 32), leading- and lagging-strand polarities (10, 24, 26), and nascent-strand size and/or abundance measurements (44) are all compatible with two preferred sites or zones of initiation (termed ori-β and ori-γ [32]) that are separated by about 22 kb and that lie in the 55-kb spacer region between the DHFR and 2BE2121 genes (Fig. 1A) (1, 32). In contrast, both neutral/neutral (5) and neutral/alkaline (40) two-dimensional (2-D) gel replicon mapping methods suggest that initiation can occur at any of a large number of sites distributed throughout the 55-kb intergenic region (15, 16, 18, 45).

Since it is relatively difficult to accurately compare initiation frequencies at different genomic sites by 2-D gel techniques (5, 36), it is possible that the frequencies of initiation at ori-β and ori-γ have been greatly underestimated (10). Furthermore,

2-D gels are technically challenging, and interpretation is based on a comparison of the patterns obtained with those of well-defined replicons. It has therefore been suggested that the patterns displayed by higher eukaryotic replication intermediates may have been misinterpreted (10, 22, 36). For example, broken bubbles could migrate as single-forked structures, resulting in an underestimation of the frequency of initiations at ori-β and/or ori-γ (10). It has also been argued that the intermediates migrating at the positions of classic bubbles or single forks, in fact, may represent some other kind of replication intermediate altogether (e.g., microbubbles and/or unidirectional origins [35]).

Because of these uncertainties, and because only one (or sometimes two) of the many available replicon mapping methods is often used to identify putative origins in higher eukaryotic genomes, we believe that it is critically important to determine whether each method of analysis is valid. We have therefore characterized the intermediates that migrate to various positions on 2-D gels in an attempt to eliminate subjectivity from the interpretation of the resulting patterns.

In an accompanying study, we have shown that broken bubbles trace novel arcs on 2-D gels that are clearly distinguishable from those of canonical replication intermediates and whose shapes depend on the position of the bubble within the fragment (30a). In the present study, we have taken advantage of this phenomenon to assess the number and positions of replication start sites within a fragment from the DHFR initiation locus by a broken bubble assay. In addition, we have developed a stop-and-go-alkaline (SAGA) gel electrophoretic technique that gives detailed information about the size of nascent strands at all positions along a given arc in a neutral/neutral 2-D gel and which therefore can distinguish classic replication intermediates from each other and from several other possible

* Corresponding author. Phone: (804) 924-5858. Fax: (804) 924-1789. Electronic mail address: jlh2d@virginia.edu.
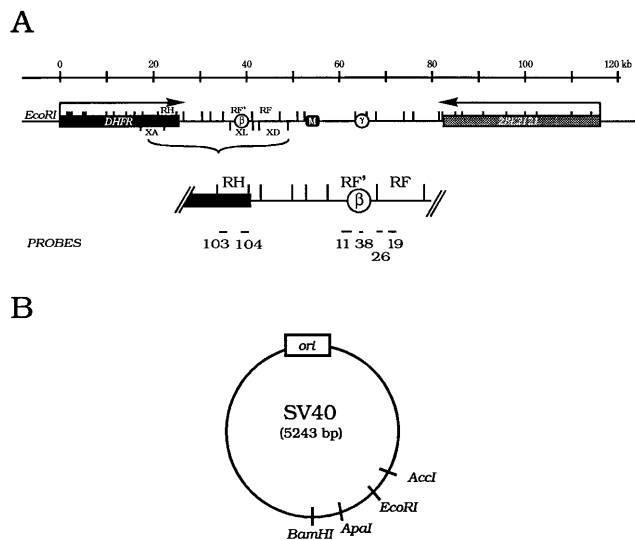
FIG. 1. Map of a 120-kb region in the 240-kb DHFR amplicon and the 5.24-kb SV40 replicon. (A) The convergently transcribing DHFR and 2BE2121 genes are indicated as boxes flanking the 55-kb intergenic region in the DHFR domain. The positions of ori-β, ori-γ, and a matrix attachment region (M) (14) are shown. Vertical lines above and below the map indicate all of the *Eco*RI sites and those *Xba*I sites relevant to this and the accompanying study (30a). Several restriction fragments are labelled to orient this map to previously published ones. A 30-kb region encompassing the 3′ end of the gene and the ori-β region are expanded to show the relative sizes and positions of hybridization probes. Details of individual probes are given in the figure legends. (B) Restriction map of the 5,243-bp SV40 replicon. The map is numbered starting at the position of the origin (nucleotide 1). Restriction sites are positioned as follows: *Eco*RI, 1782; *Acc*I, 1682; *Apa*I, 2258; *Bam*HI, 2533.

structures. When this technique is applied to the amplified DHFR locus in CHOC 400 cells, the resulting SAGA gels argue that the bubble and single-fork arcs detected in this locus on neutral/neutral 2-D gels correspond to those of the classic replication intermediates that characterize the simian virus 40 (SV40) replicon. Moreover, neither technique provides evidence for a highly preferred start site at ori-β, as has been suggested by others (10, 24, 44). Possible reasons for this discrepancy are discussed.

(This work fulfills part of the requirements for a Ph.D. in biochemistry from the University of Virginia for R. F. Kalejta.)

MATERIALS AND METHODS

Preparation of replication intermediates. SV40 replication intermediates were isolated from CV-1 cells 24 h after infection and were treated with *Bal* 31 or P1 nuclease exactly as described in the accompanying report (30a). In one experiment (see Fig. 6), SV40-infected cells were labelled 26 h after infection with [³H]thymidine (25 μCi/ml, 80 Ci/mM; Amersham Radiochemicals) and 0.2 μg of cold thymidine per ml for 10 min prior to harvesting. The methotrexate-resistant CHO cell line CHOC 400 (39) was maintained and synchronized as described previously (15). Ninety minutes after the removal of mimosine and entry into the S period, the cells were harvested and matrix-associated replication intermediates were isolated, with *Eco*RI being used to digest the DNA. As an internal control on the extent of P1 nuclease digestion in one experiment (see Fig. 4), restriction enzyme-digested SV40 replication intermediates from ∼2.5 × 10⁶ cells were mixed with CHOC 400 intermediates from ∼4 × 10⁷ cells and the mixed digest was chromatographed on benzoylated-naphthoylated-DEAE-cellulose. The caffeine wash was precipitated with ethanol, dissolved in 200 μl of Tris-EDTA, and adjusted to 50 mM sodium acetate (pH 5.5). P1 nuclease was added to 0.5 U/ml, and digestion was carried out at 37°C. At the indicated times, 50-μl aliquots were removed to a concentrated stop solution to achieve a mixture with 1.4% sodium dodecyl sulfate, 0.7 M NaCl, and 36 mM EDTA.

Electrophoresis. Standard neutral/neutral 2-D gels were run as previously described (5, 17). For SAGA gels, samples were separated by the same procedure as that of the standard neutral/neutral 2-D gel technique; the entire gel was then equilibrated in 0.4 N NaOH to denature the replication intermediates, and then the gel was subjected to two 45-min incubations with alkaline electrophore-

sis buffer (40 mM NaOH, 1 mM EDTA). The third dimension was run in this buffer in the same direction as the second dimension at ∼0.5 V/cm for 40 to 60 h at 4°C, and the buffer was changed once midway through the run.

After gel separations, replication intermediates were transferred to Hybond-N+ and hybridized with appropriate probes (see figure legends) as previously described (15). Probes were labelled with [³²P]dCTP by random priming (20). In one experiment (see Fig. 6), transfers were sprayed with En³Hance (Dupont) and fluorographed, after which the En³Hance was removed by soaking the transfers in toluene. The transfer was then hybridized with ³²P-labelled SV40 DNA.

RESULTS

Replication intermediates from the CHOC 400 DHFR intergenic region display composite patterns on neutral/neutral 2-D gels. In Fig. 2A, the classic patterns for fragments containing a centered bubble (c) and a single fork (b) are combined. Figure 2B shows the pattern displayed by a fragment containing an off-center origin. The two autoradiographs on the right (Fig. 2C and D) are examples of the patterns obtained after replication intermediates are isolated from CHOC 400 cells either at the G₁/S boundary or 100 min after the removal of mimosine and entry into the S period. In the experiment shown in Fig. 2C and D, *Eco*RI digests were hybridized with a probe specific for fragment RF′, which contains the ori-β locus (Fig. 1).

Prior to drug removal at time zero, no replication intermediates of any kind are detected in fragment RF′ (Fig. 2C). However, by 100 min, when initiation is maximal in this locus (15, 18), a typical composite pattern is detected in this fragment (Fig. 2D). What appears to be a complete bubble arc, which would normally suggest the presence of a centered replication bubble (as in Fig. 2A), is accompanied by a prominent, complete, single-fork arc. The same composite pattern is de-
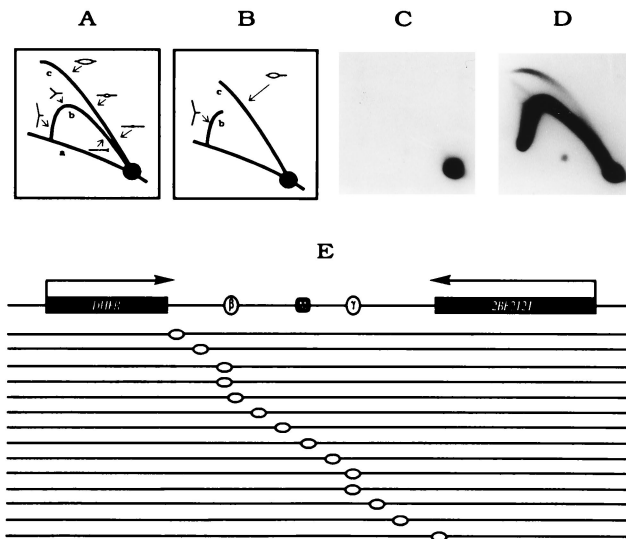
FIG. 2. Fragments from the CHO DHFR initiation locus display composite neutral/neutral 2-D gel patterns. (A) Combined bubble arc (curve c) and single-fork arc (b) patterns that characterize a classic replicon that contains a fixed, centered, bidirectional origin of replication. Curve a represents the arc of linear, nonreplicating fragments from the entire genome. (B) A bubble-to-Y transition (fork arc break) that results from an off-centered origin. (C and D) Autoradiographic patterns obtained from replication intermediates isolated from CHOC 400 cells at time zero (before the removal of mimosine) or 100 min after the release from mimosine (near the peak initiation period [15]). The ³²P-labelled hybridization probe is for *Eco*RI fragment RF′ from the initiation locus (probe 38; see the map [Fig. 1]). (E) A diagram illustrating the proposed delocalized initiation mode in the DHFR locus, in which each line below the functional map indicates different initiation site selections in different copies of the DHFR locus, with the regions around ori-β and ori-γ being somewhat preferred.
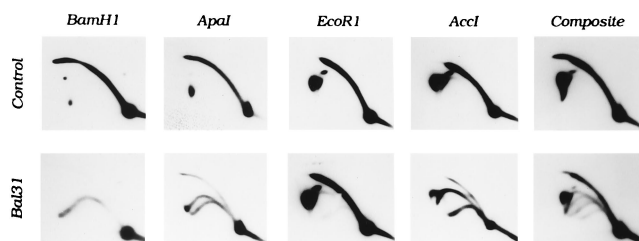
FIG. 3. Differently placed bubbles, but not their corresponding broken bubbles, comigrate on neutral/neutral 2-D gels. In the Control row, SV40 replication intermediates were digested with *Bam*HI, *Apa*I, *Eco*RI, or *Acc*I and separated on a neutral/neutral 2-D gel. In addition, approximately equal amounts of each of the four digests were mixed and separated on a gel (Composite). Transfers of the gel were probed with total SV40 DNA radiolabelled with [^{32}P]dCTP. In the *Bal* 31 row, aliquots of the same digests were subjected to partial digestion with *Bal* 31 prior to gel separation.

tected in every fragment from the 55-kb intergenic zone that has been analyzed, regardless of the restriction enzyme used to digest the DNA, although the bubble arcs are considerably stronger in fragments encompassing the central 30 to 35 kb (Fig. 1A) (15, 18).

Our interpretation of these data is diagrammed in Fig. 2E. We suggest that there are a large number of potential initiation sites in the intergenic region and that initiation occurs at different sites in different copies of the amplicon; the consequence is that any one fragment sometimes sustains an initiation event at an internal position and sometimes is replicated passively from an initiation site in another fragment in the intergenic zone. This suggestion is supported by another characteristic of neutral/neutral 2-D gel patterns for fragments from the intergenic region: in all such composite patterns and regardless of the restriction enzyme digest, the bubble arc becomes progressively less populated as it approaches the $2n$ position (i.e., comes to a point), suggesting that there are fewer very large bubbles (compare the pattern in Fig. 2D with the complete bubble arc in the *Bam*HI digest of SV40 in Fig. 3). This phenomenon can be explained by assuming that nascent strands can initiate at different positions in a given fragment in different copies of the DHFR domain and that the resulting replication bubbles comigrate on 2-D gels. However, only those initiations occurring near the center of the fragment mature to very large bubbles, since off-center origins revert to the single-fork arc when one fork crosses a restriction site (Fig. 2B).

Bubble arcs from differently placed origins, but not their corresponding broken bubble arcs, comigrate on 2-D gels. To test directly whether fragments containing differently placed origins comigrate on 2-D gels, SV40 replication intermediates were treated with *Bam*HI, *Apa*I, *Eco*RI, or *Acc*I, which cuts the genome only once at different positions (Fig. 1B). The bubble arcs from each individual digest terminate at different positions because of the transition to a termination arc when one fork crosses the nearest restriction site (see Fig. 3D in reference 30a). After the four different digests are combined, the bubble-containing fragments from each digest appear to comigrate, and the resulting bubble arc is somewhat more pointed near the $2n$ position than in any single digest (Fig. 3). Presumably, this phenomenon would have been even more exaggerated had other adventitious restriction sites made it possible to position the origin more asymmetrically. In lighter film exposures, it is clear that the bubble arcs do not precisely comigrate (data not shown), probably explaining why the bubble arcs in fragments from the DHFR initiation locus broaden as they approach the $1n$ spot (Fig. 2D) (also see references 15 and 18).

After the individual restriction digests of SV40 DNA were additionally treated with *Bal* 31, each digest produced a unique pattern of broken bubble arcs (Fig. 3), as was predicted by studies described in the accompanying report (30a). In the mixture of all four digests, the differences become even more evident (Fig. 3). Although broken bubbles from the *Bam*HI and *Eco*RI digests are relatively underrepresented in this mixture, the two sets of broken bubbles from the *Apa*I and *Acc*I digests are clearly resolved from one another, even though these digests change the position of the origin in the fragment by only 630 bp. By superimposing X-ray films of several different pairs of *Bal* 31 digests, we were able to estimate that two relatively fixed origins separated by no more than ~400 bp could be resolved. These observations form the basis of a broken bubble assay that can be used to estimate the minimum number of different bubble species that contribute to a bubble arc.

The pattern of broken bubble arcs in fragments from the DHFR initiation locus suggests random selection of nascent-strand start sites. On the basis of the results of a lagging-strand polarity assay, it has been suggested that >80% of initiations in the DHFR locus occur within a 500-bp fragment whose center is ~1.6 kb from the right end of fragment RF′ (10) (Fig. 1A). Such a preferred start site should produce broken bubble arcs with maxima at $1.49n$ and $1.17n$, with a fork arc break occurring at ~$1.52n$ (see reference 30a for the basis of the calculations). In contrast, if initiations occur at different sites in different copies of this fragment, then a collection of broken bubble arcs whose complexity would depend on the number of different start sites utilized should arise.

To discriminate between these two possibilities, *Eco*RI-digested replication intermediates were isolated from CHOC 400 cells during the peak initiation period in early S phase, and the DNA was treated in vitro with P1 nuclease to generate broken bubbles (30a). A mixture of *Apa*I- and *Acc*I-digested SV40 replication intermediates was added to the CHOC 400 sample prior to P1 digestion to serve as an internal control on the extent of single-strand-specific nuclease digestion. After separation on a neutral/neutral 2-D gel, the DNA was transferred to a membrane and hybridized first with a radiolabelled probe for fragment RF′, which contains ori-β, and subsequently with SV40 DNA. The results of two different experiments are shown in Fig. 4, in which the incubation times with the single-strand-specific nuclease are indicated.

In both experiments, and regardless of the extent of digestion, no discrete broken bubble arcs were detected in fragment RF′. Instead, there is a smear of hybridizing material underneath the fork arc that is not detectable at any film exposure in the nuclease-free controls. After the same blots were stripped and rehybridized with SV40 DNA, discrete broken bubble arcs appeared at the positions predicted by the model, demonstrating that the digestion proceeded to an appropriate extent. Note that because of inadvertent underloading of SV40 DNA in experiment 2 (Fig. 4), the resulting autoradiographic signal had to be computer enhanced.

We suggest that the smeared signals in the CHOC 400 samples represent a collection of individual broken bubble arcs arising from fragments whose individual origins occupy many different locations within the fragments and have an average spacing of less than ~400 bp. Although there could be a somewhat preferred start site at the ori-β locus in fragment RF′, it is clearly not used 80% of the time by this criterion.

SAGA gel electrophoresis. To explain the discrepancy between neutral/neutral 2-D gel results and those of other replicon mapping techniques applied to the DHFR domain, it has been suggested that the arcs we have attributed to classic

Digestion time
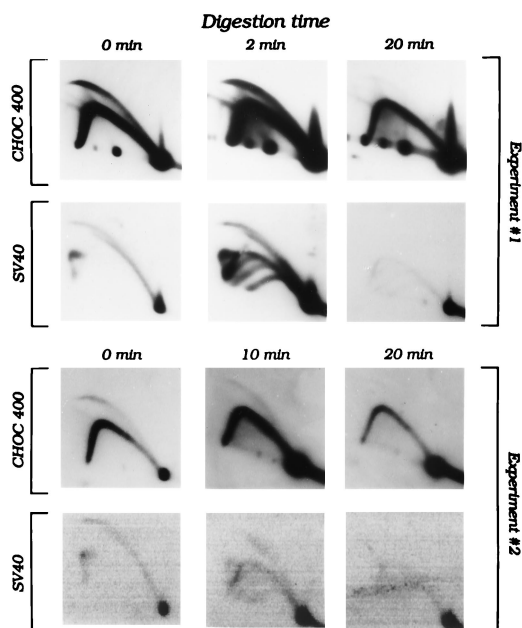
FIG. 4. The pattern of broken bubbles in fragment RF′ from the DHFR initiation locus suggests random site selection for initiation of replication. Replication intermediates from CHOC 400 cells were isolated 90 min after release from mimosine as previously described (15). A mixture of *Acc*I- and *Apa*I-digested SV40 replication intermediates were added to the CHOC 400 sample, and the preparation was digested in vitro with P1 nuclease (note that the 2-min P1 sample inadvertently contained more DNA than the other samples in experiment 1). After separation on a 2-D gel, the DNA was transferred to Hybond-N+ and hybridized with probe 38 for fragment RF′. After the CHOC 400 signals were developed, the blots were stripped and reprobed with SV40 viral DNA. In experiment 2, the film images from the viral DNA control were very weak and were therefore enhanced with the Adobe Photoshop Program.

bubbles may, in fact, represent some other kind of replication intermediate altogether (e.g., microbubbles [35]). In previous studies (18, 45), we also analyzed the DHFR locus by a complementary neutral/alkaline 2-D gel approach (40) that measures nascent-strand sizes at any position along a fragment. With the appropriate probes or probe combinations, this method can be used to determine fork direction through a fragment of interest as well as whether initiation occurs at any particular position within the fragment. After this method was applied to the amplified or single-copy DHFR domain in CHOC 400 or CHO cells, respectively, the results suggested that replication forks move in both directions throughout the intergenic region but only outward through the DHFR gene (18, 45). This result is predicted if initiation can occur at any of multiple locations in this region (Fig. 2E).

However, the neutral/alkaline gel method cannot distinguish between nascent strands arising from replication bubbles and single-forked structures of the same molecular mass in different copies of the same fragment, because they essentially comigrate on these gels (40). While a recently developed three-dimensional gel system can discriminate between the two nascent-strand species at a given molecular mass (i.e., in a given slice of the gel [33]), it would be advantageous to examine the nascent strands contained in the bubble and fork arcs across the entire size range so that any unusual replication intermediates whose structures deviate from the canonical ones might be detected (e.g., microbubbles).

We have therefore combined the neutral/neutral and neutral/alkaline gel methods into a SAGA gel technique that displays the entire spectrum of nascent strands arising from the

bubble arc or the fork arc (Fig. 5). A restriction digest of replication intermediates is first separated by the standard neutral/neutral 2-D gel method. After the second-dimension run, the entire gel is soaked in alkali to denature the parental and nascent strands, and the products are then separated in alkaline electrophoresis buffer in the same direction as the second dimension. Nascent strands (n) are released from the bubble arc (Fig. 5A), single-fork arc (Fig. 5B), or broken bubble arcs (Fig. 5C) and run as novel arcs ahead of the parental template strands (p). Since all parental strands are identically sized, they migrate the same distance in the alkaline dimension and thus maintain the approximate shape of the original double-stranded arcs (Fig. 5).

Broken bubbles also trace additional arcs on these gels because of the presence of broken parental (bp) fragments (Fig. 5). Because both branch points of small, centered bubbles are near the center of the fragment, a nick at one of these points will produce two broken parental fragments approximately one-half the length of the parental fragment. As the extent of replication increases, the branch points get farther away from the center of the fragment. Nicks occurring at these points will produce two asymmetric broken parental fragments, one slightly longer than half the parental size and one slightly shorter. This trend continues as the extent of replication increases until, at almost $2n$, one of the broken fragments is almost parental size while the other is extremely short. Thus, broken parentals would trace two arcs on SAGA gels similar to the ones observed on neutral/alkaline gels (30a). When the origin is not in the center of the fragment, two different broken bubble structures are created, each one having a unique spectrum of broken parental fragments, resulting in four novel arcs on SAGA gels (data not shown).

This technique provides a comprehensive picture of the double-stranded starting intermediate, the template (whether intact or not), and the nascent strands. Thus, it is possible to
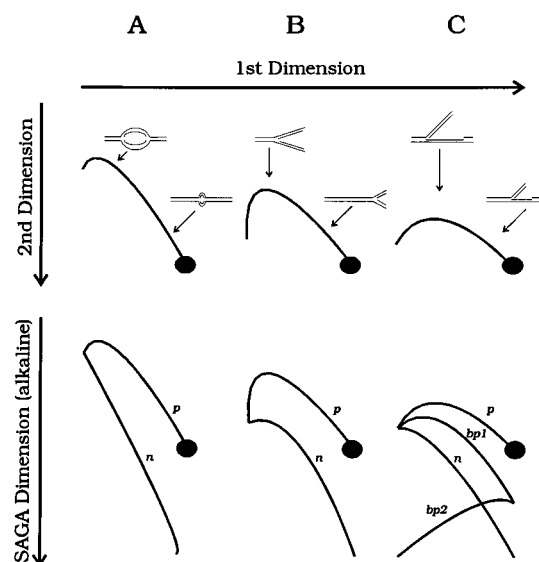
FIG. 5. Principle of the SAGA gel electrophoretic method. The first two dimensions are identical to those of standard neutral/neutral 2-D gels. The entire gel is then denatured in alkali and equilibrated and run in alkaline electrophoresis buffer in the same direction as the second dimension. All parental fragments are identical in size and maintain the shape of the original 2-D gel pattern. Since the sizes of the released nascent strands vary with the extent of replication, novel arcs are produced. Fragmented parental strands from broken bubbles also trace novel arcs on SAGA gels (see text for details).
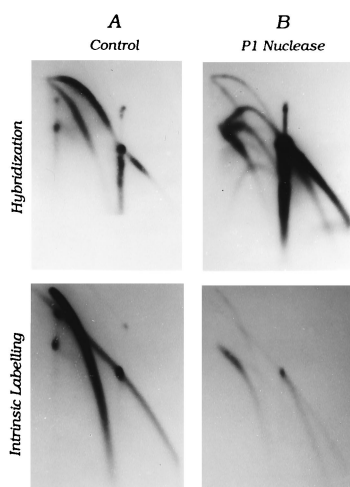
FIG. 6. Testing the SAGA gel strategy on SV40 replication intermediates. SV40 replication intermediates were labelled for 10 min in vivo with [³H]thymidine and were isolated and digested with *Bam*HI. An aliquot was additionally treated with P1 nuclease in vitro. Samples were then subjected to SAGA gel electrophoresis, blotted to HyBond-N+, and either subjected to fluorography to detect endogenous labelling of nascent strands or hybridized with ³²P-labelled total SV40 DNA. (A) Control samples showing the autoradiographic pattern resulting from the ³²P-labelled hybridization probe, which detects both parental and nascent strands (upper panel), and the intrinsic ³H-labelling pattern, which primarily illuminates nascent DNA (lower panel). (B) P1 nuclease-treated samples.

determine on a single gel the positions of internal initiation events as well as the direction of fork movement within a given fragment. Additionally, any novel intermediates whose structures deviate from what was expected (as in broken bubbles or microbubbles) should be illuminated by this gel system.

Standardizing the SAGA gel method with the SV40 replicon. SV40 viral replication intermediates were isolated and digested with *Bam*HI, which places the origin in the center of the fragment (Fig. 1B). Half of the sample was then partially digested with P1 nuclease to generate broken bubbles. After SAGA gel electrophoresis, the digests were transferred to a membrane and probed with ³²P-labelled viral DNA. The results of this analysis are shown in Fig. 6.

In the control digest (Fig. 6A), the parental template fragments maintain the shape of the original centered bubble arc (Fig. 5A [curve *p*]), while the nascent strands, as expected, trace a new arc (Fig. 5A [curve *n*]) that extends from the parental template arc all the way to the smallest detectable size. After treatment with P1 nuclease (Fig. 6B), four new arcs appear in addition to the intact parental and nascent-strand arcs from the bubble. These novel arcs arise from the broken bubble arc (30a) and consist of an intact parental strand, the short and long fragments from the nicked template (*bp1* and *bp2* in Fig. 5C), and the nascent strands. The SAGA gel patterns of both intact and nicked preparations of off-centered SV40 replication bubbles and intact replication forks were analyzed and also migrated as predicted (data not shown).

To confirm the nascent-strand assignments in these gels, SV40 replication intermediates were labelled in vivo with [³H]thymidine for 10 min prior to isolation and the intermediates were separated on a SAGA gel, transferred to a membrane, and fluorographed (Fig. 6). In control samples, the long nascent-strand arc descending from the bubble arc template, as well as a fainter signal from the arc of linears, is detected. In the sample treated with P1 nuclease (Fig. 6B), a faint intact arc arising from the bubble arc can still be discerned, but a new

nascent arc that originates at a position corresponding to that of the broken bubble arc appears (compare Fig. 6B [lower panel] and Fig. 5C [upper panel]). After removal of the fluor and probing with randomly primed SV40 DNA, patterns identical to those in Fig. 6 (upper panels) were observed (data not shown).

Analysis of replication intermediates in the CHO DHFR locus by SAGA gel electrophoresis. Thus, SAGA gel analysis has confirmed the predicted migratory behavior of SV40 replication bubbles. If the composite patterns detected in fragments from the DHFR intergenic region arise from the classic replication bubbles and forks that characterize SV40, then fragments from the DHFR locus should yield similar patterns on SAGA gels (although the patterns should again be composite). If there is a major initiation site in the ori-β locus, then the strongest nascent bubble arc should arise from fragment RF′.

Figure 7 diagrams the predicted migration patterns for a passively replicated fragment, a fragment in an initiation zone, or a fragment containing a highly preferred initiation site. Note that the entire fragment rarely can be used as a hybridization probe for fragments from mammalian genomes because of ubiquitous repetitive elements. Thus, small subfragments that are free of repetitive sequences are utilized as probes. As can be seen from Fig. 7, the autoradiographic images obtained for any given fragment depend on whether the probe comes from an end or from an internal position in the fragment, and each image provides a unique set of information.

To examine the nature of the initiation reaction in the DHFR domain, DNA from CHOC 400 cells was isolated 90 min after the removal of mimosine, at the point at which initiation is maximal, and replication intermediates were isolated, with *Eco*RI being used to digest the DNA. Part of the sample was separated on a standard neutral/neutral 2-D gel, and the remainder was separated by the SAGA gel technique. Transfers of the digests were hybridized with probes for fragment RH in the DHFR gene and fragments RF′ and RF from the intergenic region (Fig. 8) (Fig. 1 shows probe positions).

Figure 8 (top row) shows the autoradiographs obtained from the 2-D gel separations. Fragment RH from the DHFR gene displays the typical single-fork arc (Fig. 8A [top row]) expected of a fragment replicated passively by forks from an outside initiation site (presumably in the downstream intergenic zone). Figure 8B and C show the autoradiographic patterns obtained with fragments RF′ and RF, respectively; both fragments are
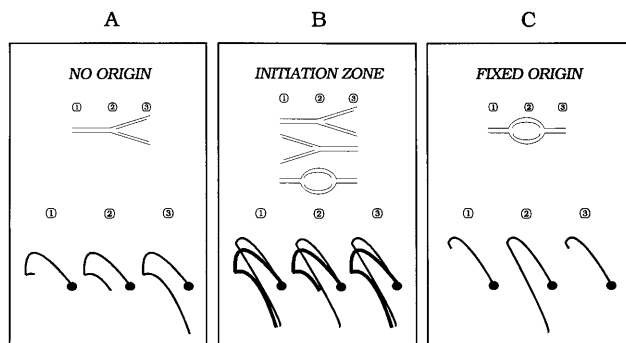
FIG. 7. Idealized SAGA patterns obtained with differently positioned probes. (A) The autoradiographic pattern that would be obtained when centered or end probes are used to analyze a fragment containing single-replication forks moving in only one direction. (B) The patterns obtained when a fragment in an initiation zone is probed with centered or end probes. (C) The patterns for a fragment containing a fixed origin.

A
(RH)

B
(RF')

C
(RF)

2-D N/N

103   11   26

3-D SAGA

103   11   26

104   38   19
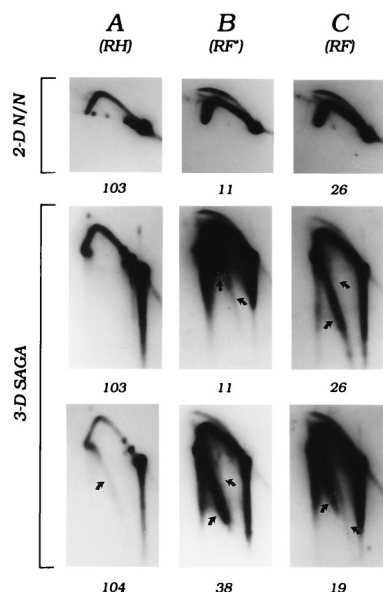
FIG. 8. Replication intermediates in the CHOC 400 DHFR domain appear to be identical to those that characterize the SV40 replicon. Replication intermediates were prepared from CHOC 400 cells 90 min after the removal of mimosine, with *Eco*RI being used to digest the DNA. Duplicate samples were separated on a standard neutral/neutral 2-D (2-D N/N) gel. One gel was then subjected to the third, alkaline dimension of the SAGA gel technique (3-D SAGA). Transfers of the gels were hybridized with probes for *Eco*RI fragments RH, RF′, and RF as follows (see the map [Fig. 1]): 103, a 1.2-kb *Eco*RI-*Xba*I fragment; 104, a 1.4-kb *Eco*RI-*Xba*I fragment; 11, a 1-kb *Pvu*II-*Bam*HI fragment; 38, a 500-bp *Pvu*II-*Xmn*I fragment; 26, an 800-bp *Hind*III-*Apa*II fragment; and 19, a 1.6-kb *Hind*III-*Kpn*I fragment. Arrows pointing to the right and left indicate nascent strands from single forks and bubbles, respectively.

6.2 kb in length and lie adjacent to one another in the intergenic region (Fig. 1A). Both display bubble arcs of nearly equal intensities as well as prominent, complete, single-fork arcs. All other fragments tested in the intergenic zone also display this pattern (15, 18). We have interpreted these composite patterns to mean that initiation can occur at different sites in the intergenic region in different copies of the DHFR domain.

The simplest SAGA gel patterns are those obtained with end probes for fragment RH (Fig. 8A [lower panels]). Since replication bubbles have never been detected in the body of the DHFR gene (15, 18, 45) and since replication forks have been shown to move only outward in the early S period in neutral/alkaline 2-D gels (18, 45), a complete arc of nascent strands emanating from the single-fork arc should be detected with an origin-proximal probe, while only the largest nascent strands should be detected with an origin-distal probe (Fig. 7A). Indeed, these patterns are obtained with probes 104 (origin proximal) and 103 (origin distal). These data confirm that forks move through RH from right to left and that the nascent strands form a monotonic series of increasing size. Note that had a probe from the central region of fragment RH been used, only those nascent strands that had passed approximately halfway through the fragment would be detected (Fig. 7A).

In both fragments RF′ and RF, the single-fork arcs release prominent nascent-strand arcs. The portion of the arc that can be detected depends on the position of the probe in the fragment, as diagrammed in Fig. 7B, but in each case extends from the full-length template size. Probe 26, which is an end probe, detects a complete diagonal, indicating that forks enter fragment RF from the left (see the map [Fig. 1A]). Additional probes (Fig. 8 and data not shown) detect dual fork directions

in RF′ and RF on SAGA gels, further arguing that ori-β is not a highly preferred initiation site. Also note that there is no indication of a broken bubble arc in either the 2-D gels or in the SAGA gels in these experiments, in agreement with the studies presented in Fig. 4 and the accompanying study (30a).

Importantly, fragments RF′ and RF from the intergenic region also display complete nascent bubble arcs with several different probes (Fig. 8B and C [lower panels]). For fragment RF′, probe 11 lies in the center of the fragment just to the left of the proposed hot spot for initiation at ori-β (10), while probe 38 encompasses the proposed hot spot; yet there is clearly very little difference in the quantities of nascent strands released from the bubble arc at the two positions. Moreover, the centered and end probes for the adjacent fragment RF also detect complete nascent arcs descending from the bubble arc. Thus, both fragments support initiation at multiple positions. Similar results were obtained with *Xba*I digests (data not shown). Furthermore, the nascent bubble arcs appear to cover the full range of fragment sizes in each case, and there is no evidence for a concentration of small nascent strands arising either from the bubble arc or fork arc that would result from microbubble formation, although a small amount of such material could obviously be missed in this analysis. Thus, we conclude that replication intermediates from the DHFR locus that migrate to the same position as SV40 bubble arcs appear in all respects to represent the canonical structures that characterize SV40 and all other replicons containing bidirectional origins that have been characterized thus far.

DISCUSSION

Neutral/neutral and neutral/alkaline 2-D gel techniques have revolutionized the study of origins of replication in eukaryotic genomes. The obvious advantage of both methods is that appropriate hybridization probes allow one to focus on the replication intermediates in a locus of interest without the interfering background of hundreds or thousands of other replicons. In addition, both methods examine extant, steady-state intermediates directly. These methods contrast with relatively indirect measurements that we and others have used and that depend on labelling with radioactive or dense precursors to specifically mark nascent DNA and then isolation and/or characterization steps that sometimes can be quite complex (1, 4, 9–11, 22–24, 28, 30–32, 38, 43, 44, 46).

The results of the 2-D gel methods for such simple replicons as those of SV40 (40), polyomavirus (45), and the yeast 2 μm circle (5) and the chromosomal replicons of yeast species (6, 7, 19, 21, 47) and cellular slime molds (2, 3) are totally consistent with those of all other methods that depend on intrinsic labelling approaches. In fact, the neutral/neutral 2-D gel system was originally standardized on highly enriched preparations of the yeast 2μm circle, and it was possible to visualize the replication intermediates constituting each arc in the gel by electron microscopy to directly ascertain their identities (5). Likewise, the neutral/alkaline 2-D gel method was originally standardized on the well-defined SV40 replicon (40).

It is only when 2-D gel techniques have been used to characterize initiation reactions in higher eukaryotic replicons that unexpected replication patterns have been observed. To our knowledge, every higher eukaryotic chromosomal locus that has been examined with neutral/neutral and/or neutral/alkaline 2-D gels displays a composite pattern of initiation similar to those that characterize the CHO DHFR locus (Fig. 2 and 8). These loci include the *Drosophila* chorion (12, 27), histone (41), and DNA polymerase-α (42) origins, a *Sciara coprophila* II9/A puff origin (34), the *Xenopus* (29) and human (37) ribo-

somal DNA initiation loci, and the Chinese hamster DHFR locus (15, 45). Recent data also indicate that the CHO rhodopsin origin is also characterized by a broad initiation zone (13a). Therefore, 2-D gel analyses suggest that in each of these cases, the choice of initiation sites is relatively distributive within large zones that range from a few to more than 50 kb in length.

Importantly, the *Drosophila* histone and DNA polymerase-α loci have also been characterized by nascent-strand size analysis, and the results of these alternative methods of analysis are consistent with the presence of large initiation zones in these loci (41, 42). However, in the case of the DHFR locus in CHO cells, the results of the 2-D gel method and several other methods of measurement do not appear to agree with one another. In particular, the results of two intrinsic labelling strategies (1, 9, 32), leading- and lagging-strand polarity assays (10, 26), and measurements of nascent-strand size and abundance (44) are consistent with the presence of at least one (ori-β) and possibly a second (ori-γ) preferred initiation site in the region between the two convergently transcribed genes in this locus. It is this dichotomy that has raised the question whether 2-D gel techniques can discriminate between the canonical mode of initiation and any unusual variation.

For that reason, we have specifically addressed the question whether the composite patterns that we and others have observed in neutral/neutral 2-D gel analyses of higher eukaryotic initiation loci represent the typical replication intermediates that characterize simple bidirectional replicons. In the accompanying study (30a), we have shown that broken bubbles are clearly distinguishable from fragments containing a single replication fork by three different criteria. It is therefore unlikely that hot spots of initiation could be missed because fragile replication bubbles are converted to single-forked broken bubbles. We also doubt that broken bubbles in preparations of replication intermediates confuse interpretation of the replication mode in any system because of their unique migration patterns on 2-D gels.

In the present study, we have taken advantage of these observations to show that the diagnostic broken bubbles indicative of a major start site are not detectable in the region of ori-β; rather, a smear of broken bubble arcs that is likely to represent a delocalized mode of initiation is observed. It could be argued that discrete broken bubble arcs were not detected because the structures that migrate as bubble arcs in neutral/neutral 2-D gels are not true replication bubbles. Therefore, they would not produce broken bubble arcs of the type that characterize fragmented SV40 replication intermediates.

To examine this possibility, we have developed a novel alkaline electrophoretic technique to determine the size of nascent strands at each point along each of the arcs detected in a neutral/neutral 2-D gel. When this SAGA gel assay is applied to the CHOC 400 DHFR locus, the nascent strands that are released from the bubble and single-fork arcs in the alkaline dimension trace continuous arcs that increase in size monotonically with the size of the starting replication intermediate. This result strongly argues that the composite patterns observed in the DHFR and other loci correspond to canonical replication bubbles and forks and not to any unusual intermediate(s). This conclusion is supported by earlier studies demonstrating the comigration of mammalian and yeast replication intermediates on 2-D gels (7) and the failure to detect any novel signals on three-dimensional gels that could correspond to fragmented replication intermediates in DNA from *S. coprophila* (33). Thus, we believe that these studies largely ruled out the possibility that the composite neutral/neutral 2-D gel

patterns observed in higher eukaryotic initiation loci have been misinterpreted. These studies also reinforce the contention that 2-D gel techniques are extremely sensitive to minor differences in the shapes and/or composition of replication intermediates (5, 40).

We do not believe that any 2-D gel method (or modification thereof) could discriminate between a zone of potential bidirectional origins and a zone of unidirectional origins, which has been invoked to explain the disparate results obtained from the DHFR locus (35). The model suggests that replication is initiated at a major bidirectional origin (ori-β) but that many secondary, unidirectional origins flanking ori-β fire concomitantly or shortly thereafter. The net result is that lagging-strand polarity would switch at the ori-β position, but replication bubbles would be detected at many positions along the template other than at ori-β; therefore, only complete bubbles, forks less than $1.5n$, and double-forked termination structures should be observed. However, we believe that this model can be ruled out because when ori-β is positioned in the center of a 4.3-kb *Xba*I fragment (fragment XL in Fig. 1A), both a bubble arc and a complete single-fork arc are observed on neutral/neutral 2-D gels (16, 18).

Why, then, do 2-D gel techniques suggest a very broad initiation zone, while several alternative methods that depend on intrinsic labelling strategies suggest narrowly circumscribed zones or sites of initiation? We believe that this dichotomy is more apparent than real and relates to the relative sensitivities and interpretations of various methods of analysis. All of the data sets can be reconciled by proposing that potential initiation sites are distributed throughout the intergenic region but that for whatever reason, the two sites at ori-β and ori-γ are somewhat preferred.

Since 2-D gel methods are extremely sensitive to even a small number of initiations, these methods will detect them wherever they occur on the template; however, they are not very good at accurately measuring absolute numbers of replication bubbles between one fragment and another, even in the same preparation of replication intermediates on the same transfer. Thus, two- to threefold differences in initiation frequencies in two different fragments could be missed.

In contrast, other methods of analysis that attempt to measure the hybridization biases of leading and lagging nascent strands or which use PCR to measure nascent-strand size and/or abundance will detect the most active start sites, but starts at other positions would probably be considered to represent background if one were expecting to uncover a relatively fixed origin. Indeed, once a preferred start site is found, the surrounding region is rarely examined for the possibility of other sites.

In fact, the DHFR locus has recently been reexamined by the lagging-strand polarity assay (23, 24), utilizing many more probes that cover a larger part of the intergenic zone (although probes for the ori-γ locus were not included). In these new analyses, it is clear that the position of the switch in lagging-strand polarity from one template to another varies from one experiment to another and, in fact, is not as dramatic as that in earlier experiments. Furthermore, in a recent study in which DNA was labelled in the first few minutes of the S period and was used as a hybridization probe on this large collection of fragments, it is clear that labelling is detected at all positions within the intergenic zone (46). These data are now largely compatible with a broad initiation zone containing two somewhat preferred regions of initiation in the ori-β and ori-γ positions. The simplest model for control of initiation in this region is that ori-β and ori-γ represent genetic replicators but that start sites can occur at distances far from the replicator.

However, it is also conceivable that these sites are preferred simply because they are situated midway between the matrix attachment region in the center of the intergenic region and the 3′ ends of the two genes (Fig. 1A). Perhaps the positive supercoiling that develops ahead of the transcription forks somehow renders the intervening region accessible to the factors that effect initiation.

On the basis of the example of the DHFR locus, we believe that it is extremely important to employ several different replicon mapping methods to identify and characterize origins of replication and to critically examine a large region encompassing a potential origin in order to gain the most complete picture of the nature of the initiation reaction. It is also clear that every technique has limitations; it is therefore important to understand what they are by continually reevaluating and improving them.

REFERENCES

1. **Anachkova, B., and J. L. Hamlin.** 1989. Replication in the amplified dihydrofolate reductase domain in CHO cells may initiate at two distinct sites, one of which is a repetitive sequence element. Mol. Cell. Biol. **9:**532–540.
2. **Benard, M., C. Lagnel, and G. Pierron.** 1995. Site-specific initiation of DNA replication within the non-transcribed spacer of Physarum rDNA. Nucleic Acids Res. **23:**1447–1453.
3. **Benard, M., and G. Pierron.** 1992. Mapping of a Physarum chromosomal origin of replication tightly linked to a developmentally-regulated profilin gene. Nucleic Acids Res. **20:**3309–3315.
4. **Braunstein, J. D., D. Schulze, T. DelGiudice, A. Furst, and C. L. Schildkraut.** 1982. The temporal order of replication of murine immunoglobulin heavy chain constant region sequences corresponds to their linear order in the genome. Nucleic Acids Res. **10:**6887–6902.
5. **Brewer, B. J., and W. L. Fangman.** 1987. The localization of replication origins on ARS plasmids in S. cerevisiae. Cell **51:**463–471.
6. **Brewer, B. J., and W. L. Fangman.** 1988. A replication fork barrier at the 3′ end of yeast ribosomal RNA genes. Cell **55:**637–643.
7. **Brun, C., P. A. Dijkwel, R. D. Little, J. L. Hamlin, C. S. Schildkraut, and J. A. Huberman.** 1995. The patterns of replication intermediates from a complex mammalian origin are identical to those of a simple origin from S. cerevisiae. Chromosoma **104:**92–102.
8. **Burhans, W. C., and J. A. Huberman.** 1994. DNA replication origins in animal cells: a question of context? Science **263:**639–640.
9. **Burhans, W. C., J. E. Selegue, and N. H. Heintz.** 1986. Isolation of the origin of replication associated with the amplified Chinese hamster dihydrofolate reductase domain. Proc. Natl. Acad. Sci. USA **83:**7790–7794.
10. **Burhans, W. C., L. T. Vassilev, M. S. Caddle, N. H. Heintz, and M. L. DePamphilis.** 1990. Identification of an origin of bidirectional DNA replication in mammalian chromosomes. Cell **62:**955–965.
11. **Carroll, S. M., M. L. DeRose, J. L. Kolman, G. H. Nonet, R. E. Kelly, and G. M. Wahl.** 1993. Localization of a bidirectional DNA replication origin in the native locus and in episomally amplified murine adenosine deaminase loci. Mol. Cell. Biol. **13:**2971–2981.
12. **Delidakis, C., and F. C. Kafatos.** 1989. Amplification enhancers and replication origins in the autosomal chorion gene cluster of Drosophila. EMBO J. **8:**891–901.
13. **DePamphilis, M. L.** 1993. Origins of DNA replication that function in eukaryotic cells. Curr. Opin. Cell Biol. **5:**434–441.
13a.**Dijkwel, P. A., and J. D'Anna.** Unpublished data.
14. **Dijkwel, P. A., and J. L. Hamlin.** 1988. Matrix attachment regions are positioned near replication initiation sites, genes, and an interamplicon junction in the amplified dihydrofolate reductase domain of Chinese hamster ovary cells. Mol. Cell. Biol. **8:**5398–5409.
15. **Dijkwel, P. A., and J. L. Hamlin.** 1992. Initiation of DNA replication in the dihydrofolate reductase locus is confined to the early S period in CHO cells synchronized with the plant amino acid mimosine. Mol. Cell. Biol. **12:**3715–3722.
16. **Dijkwel, P. A., and J. L. Hamlin.** 1995. The Chinese hamster dihydrofolate reductase origin consists of multiple potential nascent-strand start sites. Mol. Cell. Biol. **15:**3023–3031.
17. **Dijkwel, P. A., J. P. Vaughn, and J. L. Hamlin.** 1991. Mapping of replication initiation sites in mammalian genomes by two-dimensional gel analysis: stabilization and enrichment of replication intermediates by isolation on the nuclear matrix. Mol. Cell. Biol. **11:**3850–3859.
18. **Dijkwel, P. A., J. P. Vaughn, and J. L. Hamlin.** 1994. Replication initiation sites are distributed widely in the amplified CHO dihydrofolate reductase domain. Nucleic Acids Res. **22:**4989–4996.
19. **Dubey, D. D., J. Zhu, D. L. Carlson, K. Sharma, and J. A. Huberman.** 1994. Three ARS elements contribute to the ura4 replication origin region in the fission yeast, Schizosaccharomyces pombe. EMBO J. **13:**3638–3647.
20. **Feinberg, A. P., and B. Vogelstein.** 1983. A technique for radiolabeling DNA restriction endonuclease fragments to high specific activity. Anal. Biochem. **132:**6–13.
21. **Ferguson, B. M., B. J. Brewer, A. E. Reynolds, and W. L. Fangman.** 1991. A yeast origin of replication is activated late in S phase. Cell **65:**507–515.
22. **Giacca, M., L. Zentilin, P. Norio, S. Diviacco, D. Dimitrova, G. Contreas, G. Biamonti, G. Perini, F. Weighardt, S. Riva, and A. Falaschi.** 1994. Fine mapping of a replication origin of human DNA. Proc. Natl. Acad. Sci. USA **91:**7119–7123.
23. **Gilbert, D. M., H. Miyazawa, and M. L. DePamphilis.** 1995. Site-specific initiation of DNA replication in Xenopus egg extract requires nuclear structure. Mol. Cell. Biol. **15:**2942–2954.
24. **Gilbert, D. M., H. Miyazawa, F. S. Nallaseth, J. M. Ortega, J. J. Blow, and M. L. DePamphilis.** 1993. Site-specific initiation of DNA replication in metazoan chromosomes and the role of nuclear organization. Cold Spring Harbor Symp. Quant. Biol. **58:**475–485.
25. **Hamlin, J. L., P. J. Mosca, and V. V. Levenson.** 1994. Defining origins of replication in mammalian cells. Biochim. Biophys. Acta **1198:**85–111.
26. **Handeli, S., A. Klar, M. Meuth, and H. Cedar.** 1989. Mapping replication units in animal cells. Cell **57:**909–920.
27. **Heck, M. M., and A. C. Spradling.** 1990. Multiple replication origins are used during Drosophila chorion gene amplification. J. Cell Biol. **110:**903–914.
28. **Heintz, N. H., and J. L. Hamlin.** 1982. An amplified chromosomal sequence that includes the gene for dihydrofolate reductase initiates replication within specific restriction fragments. Proc. Natl. Acad. Sci. USA **79:**4083–4087.
29. **Hyrien, O., and M. Mechali.** 1993. Chromosomal replication initiates and terminates at random sequences but at regular intervals in the ribosomal DNA of Xenopus early embryos. EMBO J. **12:**4511–4520.
30. **James, C. D., and M. Leffak.** 1986. Polarity of DNA replication through the avian alpha-globin locus. Mol. Cell. Biol. **6:**976–984.
30a.**Kalejta, R. F., and J. L. Hamlin.** 1996. Composite patterns in neutral/neutral two-dimensional gels demonstrate inefficient replication origin usage. Mol. Cell. Biol. **16:**4915–4922.
31. **Kelly, R. E., M. L. DeRose, B. W. Draper, and G. M. Wahl.** 1995. Identification of an origin of bidirectional DNA replication in the ubiquitously expressed mammalian CAD gene. Mol. Cell. Biol. **15:**4136–4148.
32. **Leu, T. H., and J. L. Hamlin.** 1989. High-resolution mapping of replication fork movement through the amplified dihydrofolate reductase domain in CHO cells by in-gel renaturation analysis. Mol. Cell. Biol. **9:**523–531.
33. **Liang, C., and S. A. Gerbi.** 1994. Analysis of an origin of DNA amplification in Sciara coprophila by a novel three-dimensional gel method. Mol. Cell. Biol. **14:**1520–1529.
34. **Liang, C., J. D. Spitzer, H. S. Smith, and S. A. Gerbi.** 1993. Replication initiates at a confined region during DNA amplification in Sciara DNA puff II/9A. Genes Dev. **7:**1072–1084.
35. **Linskens, M. H., and J. A. Huberman.** 1990. The two faces of higher eukaryotic DNA replication origins. Cell **62:**845–847.
36. **Linskens, M. H., and J. A. Huberman.** 1990. Ambiguities in results obtained with 2D gel replicon mapping techniques. Nucleic Acids Res. **18:**647–652.
37. **Little, R. D., T. H. Platt, and C. L. Schildkraut.** 1993. Initiation and termination of DNA replication in human rRNA genes. Mol. Cell. Biol. **13:**6600–6613.
38. **Ma, C., T.-H. Leu, and J. L. Hamlin.** 1990. Multiple origins of replication in the dihydrofolate reductase amplicons of a methotrexate-resistant Chinese hamster cell line. Mol. Cell. Biol. **10:**1338–1346.
39. **Milbrandt, J. D., N. H. Heintz, W. C. White, S. M. Rothman, and J. L. Hamlin.** 1981. Methotrexate-resistant Chinese hamster ovary cells have amplified a 135-kilobase-pair region that includes the dihydrofolate reductase gene. Proc. Natl. Acad. Sci. USA **78:**6043–6047.
40. **Nawotka, K. A., and J. A. Huberman.** 1988. Two-dimensional gel electrophoretic method for mapping DNA replicons. Mol. Cell. Biol. **8:**1408–1413.
41. **Shinomiya, T., and S. Ina.** 1993. DNA replication of histone gene repeats in Drosophila melanogaster tissue culture cells: multiple initiation sites and replication pause sites. Mol. Cell. Biol. **13:**4098–4106.
42. **Shinomiya, T., and S. Ina.** 1994. Mapping an initiation region of DNA replication at a single-copy chromosomal locus in Drosophila melanogaster cells by two-dimensional gel methods and PCR-mediated nascent-strand

analysis: multiple replication origins in a broad zone. Mol. Cell. Biol. **14:** 7394–7403.

43. **Vassilev, L., and E. M. Johnson.** 1990. An initiation zone of chromosomal DNA replication located upstream of the c-*myc* gene in proliferating HeLa cells. Mol. Cell. Biol. **10:**4899–4904.

44. **Vassilev, L. T., W. C. Burhans, and M. L. DePamphilis.** 1990. Mapping an origin of DNA replication at a single-copy locus in exponentially proliferating mammalian cells. Mol. Cell. Biol. **10:**4685–4689.

45. **Vaughn, J. P., P. A. Dijkwel, and J. L. Hamlin.** 1990. Replication initiates in a broad zone in the amplified CHO dihydrofolate reductase domain. Cell **61:**1075–1087.

46. **Wu, J. R., and D. M. Gilbert.** 1996. A distinct G_1 step required to specify the Chinese hamster DHFR replication origin. Science **271:**1270–1272.

47. **Zhu, J., C. S. Newlon, and J. A. Huberman.** 1992. Localization of a DNA replication origin and termination zone on chromosome III of *Saccharomyces cerevisiae*. Mol. Cell. Biol. **12:**4733–4741.